Carbon, Vol. 31, No. 1, pp. 195–200, 1993
Printed in Great Britain.

0008-6223/93 $6.00 + .00

ADSORPTION RATE COEFFICIENTS FOR GASES AND VAPORS ON ACTIVATED CARBONS

GERRY O. WOOD and J. F. STAMPFER
Industrial Hygiene and Safety Group, Mail Stop K-486, Los Alamos National Laboratory, Los Alamos, NM 87545, U.S.A.

(*Received* 14 *May* 1992; *accepted in revised form* 25 *August* 1992)

Abstract—In order to estimate carbon bed breakthrough time (service life) for a given gas or vapor which is removed from flowing air by physical adsorption, both the adsorption capacity and adsorption rate need to be known. These parameters are available for only a small number of compounds at limited sets of conditions. For 27 hydrocarbons and fluorocarbons, 165 breakthrough curves were measured and analyzed to obtain adsorption rate coefficients. Reciprocals of rate coefficients at 1 and 10% of challenge breakthrough were linear functions of reciprocals of molar polarizations. Another database of breakthrough curves for 121 compounds determined at the Lawrence Livermore National Laboratory in the 1970s was also analyzed. Effects of linear flow velocity on adsorption rate coefficients were determined. Combining these two databases of 679 breakthrough curves for 147 compounds gave correlations of reciprocal adsorption rate coefficients as functions of molar polarization, linear airflow velocity, and breakthrough fraction. Only data for dry conditions and 2-cm deep beds have been considered so far.

Key Words—Adsorption, rates, vapors, gases, carbon.

1. INTRODUCTION

Activated carbon is widely used for removing gases and vapors from air. Packed beds of activated carbon granules range from air sampling tubes, to respirator cartridges, to large industrial effluent filters. Efficiencies and service lives of such carbon beds need to be known for application, design, and maintenance decisions. These performance characteristics depend on (1) the capacities of the carbon for the gases/vapors in the air, and (2) the rates of adsorption or reactive removal of these gases/vapors from the flowing air. (The term "vapor" is used for a gaseous form of a compound that also exists as a liquid or solid at ordinary temperatures and pressures.) Capacities and rates, in turn, depend on other parameters, such as temperature, concentrations, bed geometry, airflow rate, carbon particle size, carbon condition, and reactivity (physical or chemical) with the carbon surfaces.

How do adsorption capacities and rates vary from compound to compound? This is an important question because adsorption on carbon and in packed beds can't be tested for every compound. Usually, only one compound is used to characterize adsorption and to qualify a carbon or carbon bed. The conditions of such tests are also necessarily limited by time and cost constraints. Correlations of activated carbon adsorption capacities for vapors and correlations of the parameters describing them were reported previously[1]. The objective of this follow-up study was to similarly correlate adsorption rates. When combined, these correlations allow service life predictions and extrapolations to untested compounds and conditions.

2. BACKGROUND

The "ideal" reaction kinetic equation[2] (which reduces to the modified Wheeler equation[3] at small breakthroughs) is often used to describe carbon bed breakthrough and to calculate breakthrough times:

$$t_h = \frac{W_e W}{C_0 Q} - \frac{W_e \rho_\beta}{k_v C_0} \ln\left[\frac{(C_0 - C_x)}{C_x}\right], \qquad (1)$$

where

t_h = time (min) at which penetration fraction $b = C_x/C_0$ is reached,
C_0 = bed inlet concentration (ppm),
C_x = bed exit concentration (ppm),
Q = volumetric flow rate (cm^3/min),
W = weight of carbon adsorbent (g_c),
ρ_β = bulk density of the packed bed (g_c/cm^3),
W_e = adsorption capacity (g/g_c), and
k_v = adsorption rate coefficient (min^{-1}).

Several researchers have studied the parameters which affect adsorption rate coefficients. Wheeler[4] showed theoretically that when external mass transfer by diffusion through the gas phase to the surface is rate limiting, the rate constant for gas removal from the flowing phase, k_v, can be expressed as:

$$k_v(s^{-1}) = 10(v_L/Md_p^3P_T)^{1/2}, \qquad (2)$$

where v_L (cm/s) is the linear velocity, M (g/mol) is the average molecular weight, P_T (atm) is the pressure of the flowing gas, and d_p (cm) is the sorbent particle diameter. When, on the other hand, there is another

(intrinsic) rate determining step (e.g., internal diffusion) with a rate coefficient k_i of comparable magnitude to k_c, the experimental rate coefficient k_v is given[4] by:

$$k_v = k_i/(1 + k_i/k_c). \quad (3)$$

Jonas and Rehrmann, using benzene[5] and dimethyl methylphosphonate[6] vapors, observed airflow velocity dependences of k_v consistent with eqn (3) with k_c expressed as exponential functions of v_L. Deitz[7] and Wood and Moyer[8] observed approximately square root dependences of k_v versus v_L with methyl iodide and acetone, respectively. The latter are consistent with eqn (2) and external mass transfer as the rate determining step. All four studies covered overlapping airflow velocity ranges and similar carbon particle sizes. Since different velocity dependences were observed, there must be other parameter(s) involved in determining velocity dependence of k_v.

The effect of vapor type on observed adsorption rate coefficients k_v has also been studied. Jonas and Rehrmann[3] observed adsorption rate coefficients varying randomly from 20631 to 27991 min^{-1} for five gases and vapors ranging in molecular weights from 61 to 140. In other studies[9,10] it was assumed that the rate-controlling step for adsorption was internal diffusion and the rate coefficient was, therefore, proportional to the inverse square root of molecular weight M_w:

$$k_v = k'M_w^{-1/2}. \quad (4)$$

Experimental rate coefficients, ranging from 735 to 1251 min^{-1}, were reasonably consistent with eqn (4) for sets of 7 to 8 compounds ranging in molecular weights from 53 to 154.

Rehrmann and Jonas[6] also reported effects of carbon particle diameters on k_v. Semilog plots of k_v versus $1/d_p$ were almost linear up to about 30,000 min^{-1}, implying $k_v = a_1 \exp[a_2/d_p]$, rather than the relationship in eqn (2). Intercepts $\ln(a_1)$ increased with airflow velocity, but slopes a_2 remained relatively constant. At the highest airflow velocities and smallest particle sizes, the rate coefficients converged to 156,000 min^{-1}, which would be the intrinsic rate coefficient in eqn (3). Danby *et al.*[11] observed that plots of carbon tetrachloride breakthrough time versus average particle diameters were linear for five gas/carbon combinations. However, Danby also observed that capacity (slope of breakthrough time versus bed depth) increased with decreasing particle size, which suggests an inferior activated carbon for which the interior pores were accessible only by increasing the surface area. Rehrmann and Jonas[6] saw no such effect on capacity.

3. EXPERIMENTAL

Packed beds of 12 × 30 mesh (1.14 mm average granule diameter) Whetlerite (ASC) carbon were challenged with air containing the gases and vapors of liquids listed in Table 1. Although bed depth, relative humidity of the air, and, in a few cases, airflow velocity were varied, only the 165 experiments at the following conditions are considered in this paper:

2-cm bed depth; 2.3-cm bed diameter; 4.55-g carbon; 3% relative humidity air at 23 ± 2 °C; 340, 680, and 1360 ppm(v) concentrations in air; 740 cm/min airflow velocity.

At least duplicate experiments were done for each compound and concentration. The carbon was packed in stainless steel tubes.

Selected concentrations were prepared by adding the compounds to air flowing through a 1.2-cm diameter manifold. Air and gas flows were controlled and monitored with calibrated mass flow controllers (Brooks Instruments, Hatfield, PA). Liquid compounds were injected into the air stream using a calibrated syringe pump (Sage Instruments, Cambridge, MA) and vaporized. Portions of the prepared gas mixture were drawn at 3.1 L/min from the manifold through each of up to six tubes containing the carbon samples, through calibrated rotometers, and through control valves into a vacuum manifold.

Effluents from each tube along with challenge and clean air were sampled independently and sequentially. At selected time intervals these samples were drawn through a stainless steel capillary tube into the ion source of a mass spectrometer (Hewlett Packard 5995C, bypassing the gas chromatograph component) for analysis. In operation, six samples were equilibrated overnight by passing dry air through them. They were then closed off from the manifold. After the challenge concentration had been established in the air flowing through the manifold, sample tubes were opened and the challenge mixture was drawn through them. If rapid breakthrough was expected, only one tube was opened at a time and the downstream concentration monitored continuously. If slow breakthrough was expected, two tubes were run simultaneously and a switching valve diverted the effluent from either one or the other sample to the mass spectrometer detector. Interspersed with these measurements were measurements of the air used to make up the challenge and the challenge mixture itself.

The mass spectrometer was operated in the selected ion mode, monitoring the most abundant and characteristic ion of the compound being used. Since selected ion abundances were confirmed to be proportional to concentrations in air, breakthrough fractions were calculated by ion abundance ratios for the effluent samples and the challenge air samples, after subtracting the background ion abundances for the clean air samples from both. Breakthrough curves were obtained by plotting such breakthrough fractions versus time of sampling.

4. DATA ANALYSIS

Entire breakthrough curves were fit by standard least squares methods to the following mathematical equation[12] to obtain the curve centroids A:

Table 1. Challenge compounds, molecular properties, and rate coefficients

Compound	Molecular weight (g/mole)	Molar polarization (cm^3/mole)	Average rate coefficients (min^{-1}) at breakthrough	
			1%	10%
Ethene	28	10.726	2090	1200
Propyne	40	15.589	1850	1730
Propene	42	15.791	2030	1520
1,3-Butadiene	54	22.460	3680	2900
2-Butyne	54	18.644	2620	2010
1-Butene	56	22.665	3220	2850
2-Butene	56	21.656	3310	2930
Isobutene	56	22.517	4860	3920
Butane	58	20.632	4060	3250
1,1-Difluoroethene	64	10.290	2420	1290
3-Methyl-1-butene	70	24.942	3640	3190
Benzene	78	26.259	4440	4020
Trifluoroethene	82	10.072	2130	1370
1,1,1-Trifluoroethane	84	10.632	2150	1650
3,3,3-Trifluoropropyne	94	14.935	2110	1630
3,3,3-Trifluoropropene	96	15.137	2620	2380
1-Heptene	98	34.136	3760	3140
Perfluoroethene	100	9.854	2000	1310
2-Trifluoromethylpropene	110	21.863	3600	3440
Pentafluoroethane	120	10.196	1790	1500
1,1,3,3,3-Pentafluoropropene	132	14.701	2570	2010
Perfluoropropene	150	14.483	2450	1900
Perfluoro-2-butyne	162	17.336	2040	1940
Perfluorocyclobutene	162	19.301	2420	1770
3,3,4,4,4-Pentafluoro-1-butene	182	21.575	3110	2760
Perfluoro-2-butene	200	19.912	2670	2660
Perfluoro-1-heptene	278	31.084	3760	3120

$$C_x/C_0 = \frac{\exp[(t_b - A)/(B + G(t_b - A))]}{\exp[(t_b - A)/(B, + G(t_b - A))] + (1 - P_x)/P_x}, \quad (5)$$

where P_x is the breakthrough fraction at the curve centroid and A, B, and G are adjustable parameters. This equation is an extension of eqn (1) to account for the usually observed asymmetry of breakthrough curves. A fourth parameter, H, used in Ref. [12] was not needed for fitting these breakthrough curves. On the time axis these centroids correspond to stoichiometric times and are related to equilibrium capacities[13].

Gary Nelson provided breakthrough curve data and calculated time centroids [14] not previously published for experiments done at the Lawrence Livermore National Laboratory in the 1970s[15]. These studies included 121 compounds, 3 carbons, and a variety of challenge concentrations, airflow velocities, and relative humidities. Respirator canister bed depths were all about 2 cm. Only data for experiments at relative humidities at or below 50% were considered in this paper. Effects of higher humidities will be addressed later.

Times at which 1 and 10% of challenge concentration breakthroughs occurred were obtained from interpolations of experimental data from both our and the Livermore studies. The first term of eqn (1) represents stoichiometric time t_{sto}. Differences between breakthrough times and t_{sto} were used to calculate reciprocals of apparent adsorption rate coefficients for bed volumes $V_\beta = W/\rho_\beta$ at the selected penetration percents, $b = 100\%\ C_x/C_0$, using this rearrangement of eqn (1):

$$\frac{1}{k_{vb}} = \frac{V_\beta(t_{sto} - t_b)}{Qt_{sto}\ \ln[(C_0 - C_x)/C_x]}. \quad (6)$$

The k_{vb} are called "apparent" rate coefficients, since few of the experimental breakthrough curves were ideally symmetrical with stoichiometric times at $C_x/C_0 = 0.5$. Reciprocals of k_{vb} were used for correlations since this is the function appearing in eqn (1), which is used for calculations of service life (breakthrough time).

Data were fit to correlation equations (below) using the nonlinear curve fitting module of a commercial program, SYSTAT (SYSTAT, Inc., Evanston, IL), on a PC-compatible 386SX computer.

5. CORRELATIONS OF EXPERIMENTAL RATE COEFFICIENTS

Our data from 165 experiments with 27 hydrocarbons and fluorocarbons (Table 1) covered a wide range of compounds: from ethene and 1,1-difluoroethene to 1-heptene and perfluoro-1-heptene. Since rate coefficients were observed to be independent of gas/vapor concentration, we averaged their reciprocals for each compound. First, we attempted correlations of average reciprocal rate coefficients with molecular weights. Figure 1 shows a plot of av-

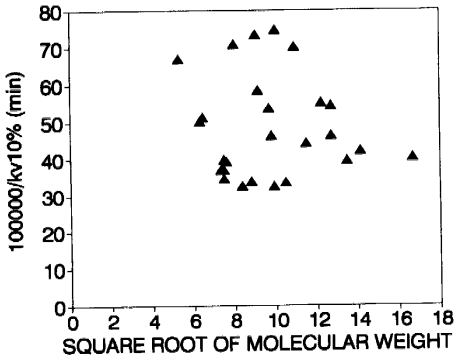

Fig. 1. Variation of reciprocal rate coefficients at 10% breakthrough with square roots of molecular weights. Hydrocarbons and fluorocarbons.

erage 10% reciprocal rate coefficients versus square roots of molecular weights. There was no apparent trend with this or any other function of molecular weight alone. Rate coefficients from 1% breakthrough data led to the same conclusion.

Next, in analogy with capacity[1], we attempted correlations with molar polarization P_c, defined by:

$$P_c\,(\mathrm{cm^3/mole}) = \frac{n_D^2 - 1}{n_D^2 + 2}\frac{M_w}{d_L}. \qquad (7)$$

Refractive index n_D, and liquid density d_L, can be taken from a standard handbook[16] for common liquids. Molar polarizations for liquids and gases without these data can be easily calculated using additive structural contributions[16]. Alternatively, molar polarizations can be obtained from tabulated values of average experimental electric dipole polarizabilities by dividing the latter by the conversion constant $0.3964308 \times 10^{-24}$ cm^3[16].

Figure 2 shows the average reciprocal rate coefficients at 10% breakthrough to be a linear function of the reciprocal molar polarizations:

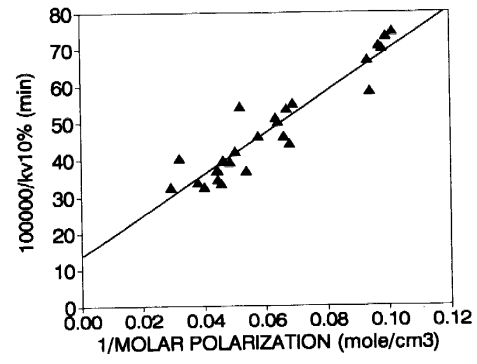

Fig. 2. Variation of reciprocal rate coefficients at 10% breakthrough with reciprocal molar polarization. Hydrocarbons and fluorocarbons.

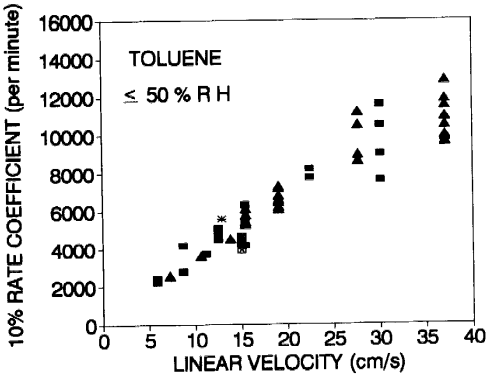

Fig. 3. Effect of linear airflow velocity on toluene adsorption rate coefficients at 10% breakthrough. The four symbols represent four different carbons used by Nelson *et al.* (refs. [14–15,17]).

$$1/k_{vb} = I + S_b(1/P_c). \qquad (8)$$

Such a plot from data at 1% breakthrough appeared to have the same intercept I, but a different slope S_b. When all data (not just averages) were fit to eqn (8), the common intercept was $I = 1.32 \times 10^{-4}$ min and the slopes were $S_{1\%} = 4.01 \times 10^{-3}$ min-cm^3/mol and $S_{10\%} = 5.67 \times 10^{-3}$ min-cm^3/mol. The statistically different slopes reflect the observed asymmetry of most of the breakthrough curves. Both sets of data were combined into one empirical equation, which can be used for interpolating to intermediate breakthrough percents:

$$S_b = (0.00719) - (0.00069)\ln((C_0 - C_x)/C_x). \qquad (9)$$

The overall relative standard deviation of 330 individual $1/k_{vb}$ data from eqn (9) was 7.7×10^{-5} min.

The Livermore experiments covered a range of airflow velocities, allowing observation of airflow velocity effects. Figure 3 shows an increase in the toluene 10% rate coefficient with linear airflow velocity for three carbons. Again, the 1% rate coefficients followed the same pattern as the 10% ones. Other compounds (acetone, ethyl acetate, 2-butanone, benzene, and methyl chloroform) also showed initial linear increases of k_{vb} with flow velocity and a tendency to level off at higher velocities v_L, according to the function:

$$k_{vb} = (z_a v_L)/(1 + z_2 v_L). \qquad (10)$$

The best value of z_2 for all 706 data (1 and 10% times) for 121 compounds was $z_2 = 0.027$ s/cm, producing a standard deviation of 70 min^{-1} in k_{vb}.

6. CONSOLIDATION OF BOTH DATA SETS

With the molar polarization and flow velocity dependencies defined, the two data sets were compared.

Also included were Los Alamos data for four other compounds (acetone, chloroform, ethyl acetate, and diethyl ether) at dry conditions. Values of $100{,}000/z_a$ were calculated from eqn (10) using $z_2 = 0.027$ s/cm and average reciprocal rate coefficients obtained from breakthrough time measurements for each compound with four or more data. Figure 4 is a plot of these values versus reciprocal molar polarizations for the two sets of 10% breakthrough data. The Livermore data, shown in solid squares, is in good agreement with the Los Alamos data, shown in open squares, without any further adjustments. Similar agreement was observed for reciprocal 1% breakthrough rate coefficients.

Finally, all the data (not just averages of sets of four or more data) were combined. This included reciprocal rate coefficients calculated from 1 and 10% breakthrough and stoichiometric times for 203 Los Alamos breakthrough curves and 482 Livermore breakthrough curves. The logarithm of the following equation was fit to the data:

$$1/k_{vb} = ((1 + 0.027 \cdot v_L)/v_L) \cdot (I + S_b/P_c), \quad (11)$$

with the results:

$$I = 0.000825 \text{ min-(cm/s)},$$
$$S_{1\%} = 0.036 \text{ min-(cm/s)-(cm}^3\text{/mole)},$$
$$S_{10\%} = 0.050 \text{ min-(cm/s)-(cm}^3\text{/mole)}.$$

The logarithm of eqn (11) was used for curve fitting, since examination of the data showed that the relative deviation was more constant than the absolute deviation. Relative standard deviations of reciprocal rate coefficients were 24% at 1% breakthrough and 26% at 10% breakthrough. (Note: allowing z_2 to adjust in this data fit, instead of forcing it to be 0.027, did not significantly improve the data fit.) Again, for interpolation to other breakthrough percents:

$$S_b = 0.063 - 0.0058 \ln[(C_0 - C_x)/C_x], \quad (12)$$

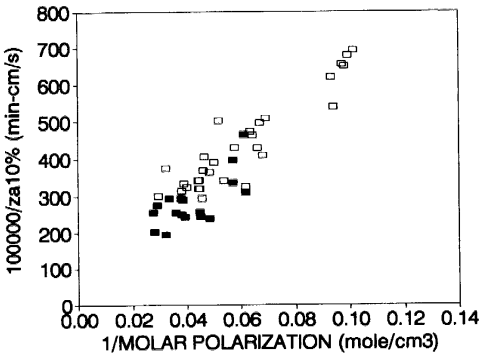

Fig. 4. Comparisons of reciprocal rate coefficient parameters for Los Alamos data (open squares) and Livermore data (solid squares) at 10% breakthrough.

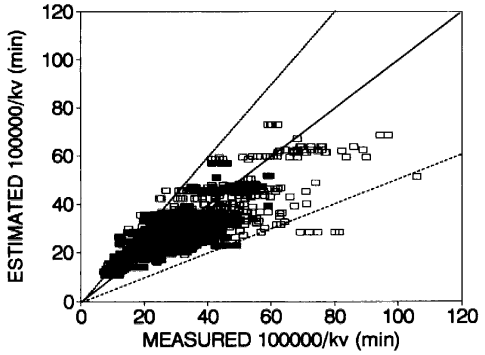

Fig. 5. Comparisons of reciprocal rate coefficients calculated by the correlation with those calculated from breakthrough curve data. Solid squares = 1% breakthrough; open squares = 10% breakthrough.

with a combined relative standard deviation of 25% in $1/k_{vb}$. Figure 5 shows a comparison of estimated and measured values of $1/k_v$ for both 1% (solid squares) and 10% (open squares) breakthroughs. The dashed lines represent two standard deviations.

7. DISCUSSION

The uncertainty in the final correlation illustrated by Figure 5 is not surprising. The rate coefficient and its reciprocal must be calculated indirectly from the difference between a measured breakthrough time and a stoichiometric time obtained from an integration of the full breakthrough curve. Both times are subject to experimental errors and their difference may be small, which magnifies the relative errors. Also, we are dealing with a heterogeneous material, carbon granules. This may result in packing variability and localized differences in adsorption properties within the packed bed. Fortunately, the kinetic contribution [second term of eqn (1)] to the breakthrough time is often smaller than the capacity contribution (first term); the error contribution of the former is, therefore, proportionately less.

Figure 1 shows that the molecular weight effect on these adsorption rate coefficients was not the predicted inverse square root function. Molar polarization was a useful property for correlating rate coefficients, as it was for correlating adsorption capacities[1]. Physically, molar polarization is a measure of the ability of an electric field to distort the electron distribution of a molecule. Such a distortion could accelerate the migration of a molecule to an adsorption site. However, it is also possible that molar polarization is related to some other molecular property that is more directly controlling the adsorption rate.

The observed velocity dependence (Fig. 3) of rate coefficients was greater than expected. Others, including this author[8] have reported a square root dependence of k_v on airflow rate (or velocity). More

complicated dependences have also been reported[5,6] as discussed above. At this point there is no good explanation for the differences in these observations.

Also puzzling, and perhaps related, was the apparent lack of particle size dependence of the adsorption rate coefficients. The three carbons in the Livermore studies had average particle sizes of 0.123, 0.135, and 0.177 cm[17], but indistinguishable rate coefficients. The carbon used in the Los Alamos studies had an average particle size of 0.105 cm, but gave rate coefficients in good agreement with those from the Livermore data. In apparent contrast, two other studies[6,11] have shown clear influences of particle sizes on adsorption rates. The explanation may be that in the latter studies, the particle size ranges of the samples of differing average sizes were relatively small. In commercial carbons with wider carbon mesh ranges, it may be the dominant or largest size particle that is critical, rather than the average size.

8. APPLICATIONS

Carbon bed breakthrough times (service lives) can be estimated using eqn (1), k_v estimates from eqns (11) and (12), and W_e estimates from eqns (5) and (6) in Ref. [1]. Combined uncertainties of such a calculation due to uncertainties in $1/k_v$ (σ = 25%) and W_e (σ = 0.029 g/g$_c$) depend on the relative contributions of the two terms in eqn (1). Micropore volume and molar polarization would also be input values.

If there are some experimental data available for the carbon or carbon bed, these estimates can be made more reliable. For example, measuring an ethyl acetate breakthrough curve would allow calculation of a reference reciprocal rate coefficient by eqn (6). The reciprocal rate coefficients for an untested compound, such as benzene, could then be obtained by ratios using eqn (11), airflow velocities, and molar polarizations of the two compounds. If the flow velocities were the same, they would cancel out in such a ratio. In addition, the ethyl acetate stoichiometric time, obtained from integrating or fitting the breakthrough curve [e.g., eqn (5)], would provide a micropore volume to use for the benzene calculation[1].

REFERENCES

1. G. O. Wood, *Carbon* **30**, 593 (1992).
2. T. Vermeulen, M. D. LeVan, N. K. Heister, and G. Klein, *Perry's Chemical Engineers Handbook* (Edited by R. H. Perry, *et al.*), 6th edn, Section 16. McGraw-Hill, New York (1984).
3. L. A. Jonas and J. A. Rehrmann, *Carbon* **11**, 59 (1973).
4. A. Wheeler, *Catalysis* (Edited by P. H. Emmett), Vol. II, p. 105. Reinhold, New York (1955).
5. L. A. Jonas and J. A. Rehrmann, *Carbon* **12**, 95 (1974).
6. J. A. Rehrmann and L. A. Jonas, *Carbon* **16**, 47 (1978).
7. V. R. Deitz, C. H. Blachly, and L. A. Jonas, *Nucl. Tech.* **37**, 59 (1978).
8. G. O. Wood and E. M. Moyer, *Am. Ind. Hyg. Assoc. J.* **50**, 400 (1989).
9. L. A. Jonas, Y. B. Tewari, and E. B. Sansone, *Carbon* **17**, 345 (1979).
10. C. J. Danby, J. G. Davoud, D. H. Everett, C. N. Hinshelwood, and R. M. Lodge, *J. Chem. Soc.* (London), 918 (1946).
11. E. B. Sansone, Y. B. Tewari, and L. A. Jonas, *Environ. Sci. Tech.* **13**, 1511 (1979).
12. G. O. Wood, *Proc. 1989 U.S. Army Chemical Research, Development and Engineering Center Scientific Conf. Chemical Defense Research*, 14–17 November 1989, CRDEC-SP-024, 511, Aberdeen Proving Ground, MD (1990).
13. G. O. Wood and E. S. Moyer, *Am. Ind. Hyg. Assoc. J.* **52**, 235 (1991).
14. G. O. Nelson and C. A. Harder, *Am. Ind. Hyg. Assoc. J.* **52**, 235 (1991).
15. G. O. Nelson and A. N. Correia, *Am. Ind. Hyg. Assoc. J.* **33**, 797 (1972).
16. *CRC Handbook of Chemistry and Physics* (Edited by R. C. Weast), 67th edn, E-372, E-74. CRC Press, Boca Raton, FL (1987).
17. G. O. Nelson, *Am. Ind. Hyg. Assoc. J.* **37**, 205 (1976).